X-ray absorption spectra at the Ru and Mn $L_{2,3}$ edges and long-range ferromagnetism in SrRu$_{1-x}$Mn$_x$O$_3$ solid solutions ($0 \leq x \leq 0.5$)

Ranjan K. Sahu,[1] Z. Hu,[2] Manju L. Rao,[1] S. Sundar Manoharan,[1,*] T. Schmidt,[3] B. Richter,[4] M. Knupfer,[2] M. Golden,[2] J. Fink,[2] and C. M. Schneider[2]

[1]*Materials Chemistry Laboratory, Department of Chemistry, Indian Institute of Technology, Kanpur, 208 016, India*
[2]*Institute for Solid State Research, 20 Helmholtz strasse, D-01069, Germany*
[3]*Experimentelle Physik, Universität Würzburg, D-97074 Wurzburg, Germany*
[4]*Fritz Haber Institute of the Max Plank Society, Dept. of Chemical Physics, FaradayWeg 4-6, D-14195 Berlin, Germany*

The $L_{2,3}$-edge spectra of Ru and Mn in the SrRu$_{1-x}$Mn$_x$O$_3$, $0 \leq x \leq 0.5$, system reveals the coexistence of a mixed-valence redox pair involving both Mn^{3+}/Mn^{4+} and Ru^{4+}/Ru^{5+}. This influences a long-range ferromagnetic ordering, showing a finite T_c up to 50% Mn doping at the Ru site. A crystal-field-multiplet calculation indicates that the intensity distribution of the t_{2g}- and e_g-related peaks between the Ru L_2 and Ru L_3 edges reflects the Ru valences, rather than the crystal field interactions. By comparison with the Mn $L_{2,3}$ x-ray absorption spectroscopy of the well-known Mn(III) and Mn(IV) references, the mixed-valence Mn ions in the SrRu$_{1-x}$Mn$_x$O$_3$ system are confirmed. This study forms a basis for the understanding of exchange interactions between two dissimilar transition-metal ions in the manganite crystal lattice.

I. INTRODUCTION

The mixed valency of Ru(IV)/Ru(V) in the magnetic superconductor RuSr$_2$GdCu$_2$O$_8$ (Ref. 1) and in the Ruddlesden-Popper series Sr$_{n+1}$Ru$_n$O$_{3n+1}$ ($n = 1$, 2, and ∞) manifests in showing interesting electrical and magnetic properties.[2] In SrRuO$_3$, Ru(IV) is a well-studied low-spin d^4 system, while in the higher analog Sr$_4$Ru$_2$O$_9$, Ru exists as Ru(V) with a d^3 configuration. Recently, it has been observed that Ru exhibits novel manifestations when substituted in rare-earth manganites by showing an unusual double-exchange-mediated transport behavior[3] with up to 40% Ru doping at the Mn site. Furthermore, Ru in Nd$_{0.5}$Sr$_{0.5}$MnO$_3$ (Ref. 4) is reported to significantly melt the charge ordering due to chemical pressure effects. The exact role of Ru on the magnetotransport properties is still not fully understood, although the mixed valence of Ru seems to play a vital role. To probe the existence of the valence states in Ru and to understand the role of Ru in extending the double-exchange-mediated transport properties as observed in manganites, Ln$_{0.7}$M$_{0.3}$Mn$_{1-x}$Ru$_x$O$_3$, we have chosen a simple system such as SrRu$_{1-x}$Mn$_x$O$_3$, where $0 \leq x \leq 1$. This system could offer insights on the coexistence of mixed valency, especially in a non-A-site-doped system. SrMnO$_3$ and SrRuO$_3$ are the end members of this series wherein both the transition-metal ions are in a tetravalent state. While SrMnO$_3$ is an antiferromagnetic insulator, SrRuO$_3$ is metallic, showing a ferromagnetic ordering below $T_c \sim 160$ K.[5] The saturation magnetization M_s is $(1.1-1.3)\mu_B$/Ru, and the ordered moment is reported to be $(1.4 \pm 0.4)\mu_B$/Ru as observed by neutron diffraction studies.[6]

In this paper, we first present the structural transition from tetragonal to orthorhombic symmetry with increasing Mn content and, second, we show that the ferromagnetic ordering in SrRuO$_3$ is substantial up to 50% Mn substitution at the Ru site. To understand what could probably influence this long-range ferromagnetic coupling, we study the ground-state electronic configuration of Ru and Mn in SrMnO$_3$-SrRuO$_3$ solid solutions. We observe that the redox states of the mixed-valence Ru and Mn appear near an equiatomic composition $x = 0.50$. This is in sharp contrast to our recent results on La$_{0.7}$M$_{0.3}$Mn$_{1-x}$Ru$_x$O$_3$,[7] which indicate that the pentavalent Ru begins to appear for a low doping level of Ru, in other words, when a substantial Mn(IV) concentration is present, wherein the reduction-oxidation potential of Ru(IV)/Ru(V) (1.07 eV) and Mn(III)/Mn(IV) (1.02 eV) seems to play a decisive role in balancing the charge distribution.

II. EXPERIMENT

The samples were prepared by the conventional solid-state method using high-purity SrCO$_3$, RuO$_2$, and MnO$_2$. These powders were calcined at 950 °C for 48 h, pressed into pellets, sintered in ambient atmosphere at 1200 °C with intermittent grindings, and slowly cooled at 1 °C/min in air. For an exact determination of the oxidation state in the compound it is essential to examine the reference material. In the case of ruthenium, compounds such as RuO$_2$, Sr$_4$Ru$_2$O$_9$, and La$_{2-x}$Sr$_x$Cu$_{1-y}$Ru$_y$O$_{4-\delta}$ were used as reference for Ru(IV), Ru(V), and mixed-valence Ru(IV) and Ru(V), respectively. For manganese, we have employed MnO$_2$ for Mn(IV) and LiMn$_2$O$_4$ for the mixed-valence Mn(III) and Mn(IV), respectively. All the compounds taken as reference materials were prepared under same conditions as the investigated compounds. The x-ray powder diffraction patterns for all the samples were recorded using a Rich-Seifert 3000 TT x-ray diffractometer and the lattice constants were calculated using a slow 2θ scan. EPMA was carried in order to determine the distribution of Mn and Ru ions. The magnetic measurements were done using an OXFORD vibrating sample magnetometer. The Ru $L_{2,3}$ XAS spectra of the polycrystalline SrRu$_{1-x}$Mn$_x$O$_3$ series were recorded in the transmission geometry at the EXAFS-II beamline at Hamburger Synchrotronstrahlungslabor, HASYLAB/DESY in Hamburg using a

Si (111) double-crystal monochromator. This resulted in an experimental resolution of ~1.2 eV (full width at half maximum) at the Ru L_3 threshold (2838 eV). A linear background was subtracted from the measured spectra. The Mn $L_{2,3}$ XAS data were recorded in total electron yield at the SX700-II beamline at Berliner Elektronen Speicherring fur Synchrotronstrahlung (BESSY), Berlin. The oxygen content was estimated by thermogravimetry analysis (TGA). All compounds showed the expected oxygen stoichiometry within an error of ±0.03.

III. RESULTS AND DISCUSSION

A. Structure

The strong influence of the B-site cationic mismatch on the structure is noticed as shown in Figs. 1(a) and 1(b), which consequently affects the magnetism and transport behavior. The powder x-ray diffraction patterns for $SrRu_{1-x}Mn_xO_3$, $0 \leq x \leq 0.5$, show that the compounds are highly crystalline and homogeneous, with no signature for impurity phases. The diffraction peaks for the parent compound; $SrRuO_3$ can be indexed to orthorhombic symmetry.[8] With increasing Mn doping, an overall decrease in the unit cell volume is observed up to $x \leq 0.3$. This is obvious since Mn(IV) with ionic radii of 0.52 Å compared to Ru(IV) (0.63 Å) brings about an overall cell volume contraction. For $x > 0.3$, the system goes from an orthorhombic to a more distorted orthorhombic structure as observed by Joy *et al.*,[9] which is clearly seen in the splitting of [220] reflection and a pronounced shift to lower 2θ angle for [110] reflection. This is mainly due to the redox mechanism that begins to operate at higher Mn(IV) concentration. Mn(III)/Mn(IV) having a redox potential of 1.02 eV, comparable to 1.07 eV for Ru(IV)/Ru(V), leads to a reduction of the Mn(IV) state to the Mn(III) state while Ru(IV) goes to Ru(V). This observation will be discussed further with x-ray absorption spectroscopy (XAS) data in the following section. The Mn(III) concentration, which becomes appreciable above $x = 0.3$, brings about a strong distortion in the unit cell since Mn(III, $t_{2g}^3 e_g^1$) is a Jahn-Teller ion. For an equiatomic composition, the distorted orthorhombic unit cell clearly shows splitting for the [220] reflection as shown separately in the inset in Fig. 1(a).

B. Magnetism

The magnetization curves were recorded as a function of the magnetic field and temperature. All *M-H* loops show a ferromagnetic contribution, and the loops disappear above the Curie temperature. It is noteworthy to observe that the ferromagnetism extends up to 50% of Mn doping, still with a $T_c \sim 125$ K as shown in Fig. 2(a). Figure 2(b) shows the reciprocal of the magnetic susceptibility versus temperature for $SrRu_{1-x}Mn_xO_3$, $0 \leq x \leq 0.5$, measured at 5 T. For a quantitative evaluation of the effective magnetic moment, the Curie-Weiss equation was fitted. All compositions obey the Curie-Weiss law above 200 K. We fitted the data of $\chi(T)$ between 200 and 300 K with $\chi(T) = \chi_0 + \chi_{CW}$, where χ_0 is the temperature-independent term and $\chi_{CW} = C/(T - \theta_w)$ is the temperature-dependent Curie-Weiss term. Here C is the
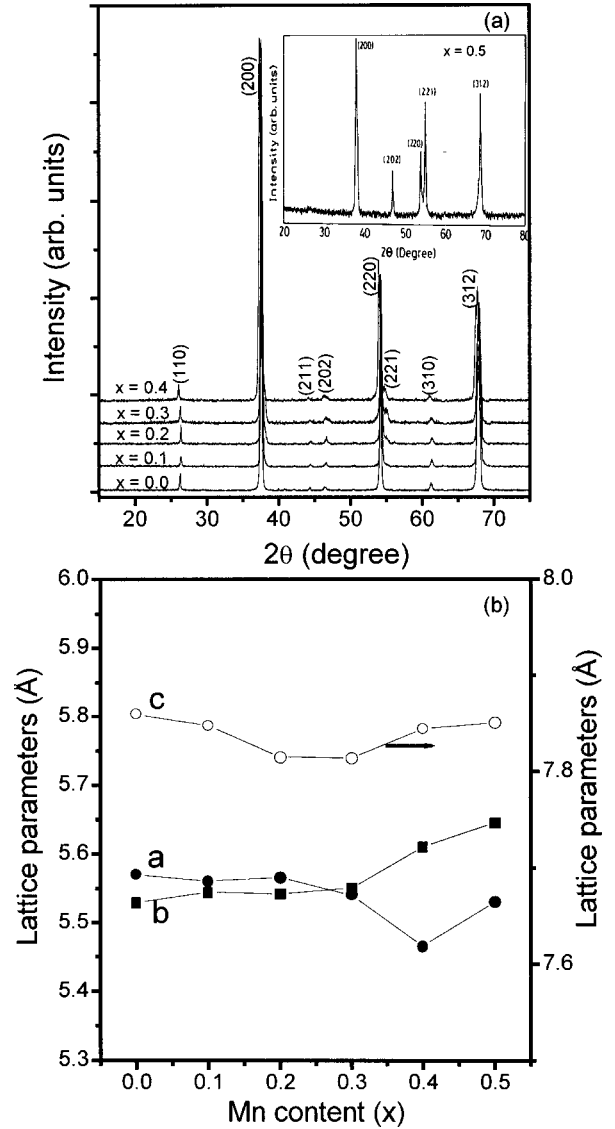

FIG. 1. (a) X-ray powder diffraction patterns of Mn-doped $SrRu_{1-x}Mn_xO_3$ recorded at room temperature using a Co $K\alpha$ source with Fe filter. (b) Room-temperature lattice constants and unit cell volume obtained from x-ray diffraction spectra of Mn-doped $SrRu_{1-x}Mn_xO_3$, $0 \leq x \leq 0.5$. A distinct increase in the unit cell volume and the structural distortion for $x > 0.3$ indicates that few percent of Mn(IV) reduce to Mn(III), having the cooperative John-teller distortion and the greater ionic radii.

Curie constant and θ_w is the Weiss temperature. The temperature-independent term χ_0 was determined within the accuracy of $\pm 5 \times 10^{-5}$ emu/mol for Ru and is included into the fits. The value of the P_{eff} (in Bohr magnetons) deduced from $C = N_A P_{eff}^2 \mu_B / 3 k_B$ (where N_A is the Avogadro number, μ_B is the Bohr magneton, k_B is the Boltzmann constant, and P_{eff} is the effective magnetic moment), the Curie constant and Weiss temperature are shown in Table I. The p_{eff} value for $SrRuO_3$ agrees well with the reported value suggesting a low-spin Ru(IV):$t_{2g}^4 e_g^0$ with $^3T_{1g}$ symmetry.[10] On doping Mn at the Ru site, the effective magnetic moment increases. These values are larger than the theoretically predicted effective magnetic moment (Table I), considering the spin-only
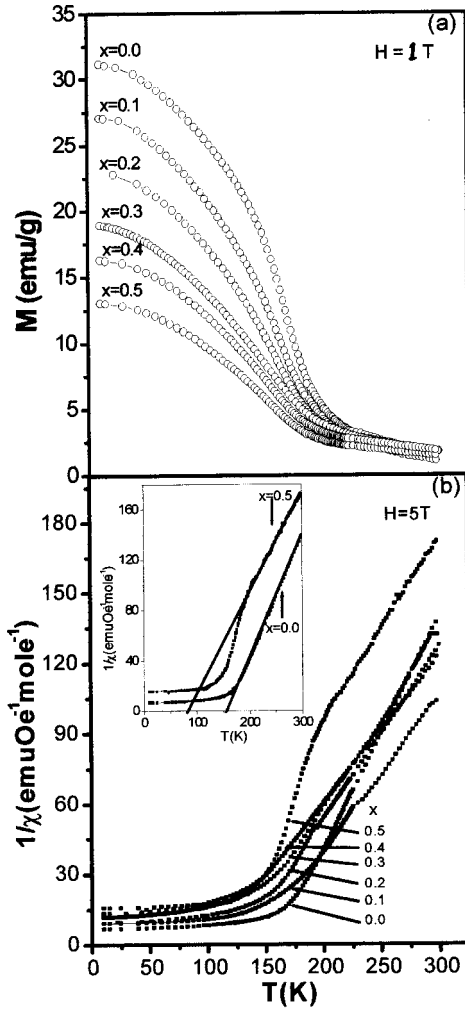
FIG. 2. (a) Magnetization as a function of temperature measured at $H = 1$ T. (b) shows the temperature dependence of the inverse magnetic susceptibility measured at 5 T for Mn-doped SrRu$_{1-x}$Mn$_x$O$_3$, $0 \leq x \leq 0.5$. The solid line shows the fit of the Curie-Weiss equation to the linear portion of the curve above 200 K [inset to (b)].

magnetic moment ($S = 1$) for low-spin Ru(IV) and ($S = 3/2$) for high-spin Mn(IV). For instance, the experimental value of p_{eff} for SrRu$_{0.9}$Mn$_{0.1}$O$_3$ is estimated to be $3.23\mu_B$, which is larger than the value of $2.95\mu_B$ expected for the

TABLE I. Some properties of the SrRu$_{1-x}$Mn$_x$O$_3$ compounds.

Composition	θ (K)	C (emu K mol^{-1} Oe^{-1})	p_{eff} (Expt.)	p_{eff} (Theory)[a]
SrRuO$_3$	160	1.01	2.83	2.83
SrRu$_{0.9}$Mn$_{0.1}$O$_3$	153	1.31	3.23	2.95
SrRu$_{0.8}$Mn$_{0.2}$O$_3$	124	1.38	3.32	3.07
SrRu$_{0.7}$Mn$_{0.3}$O$_3$	115	1.40	3.35	3.18
SrRu$_{0.6}$Mn$_{0.4}$O$_3$	105	1.57	3.54	3.29
SrRu$_{0.5}$Mn$_{0.5}$O$_3$	95	1.91	3.89	3.39

[a]p_{eff} (Theory)$= g^2[1 - x \ S_{\text{Ru}^{4+}}(S_{\text{Ru}^{4+}} + 1) + x \ S_{\text{Mn}^{4+}}(S_{\text{Mn}^{4+}} + 1)]$ x is the Mn doping concentration and $g \sim 2$ is the Lande factor.
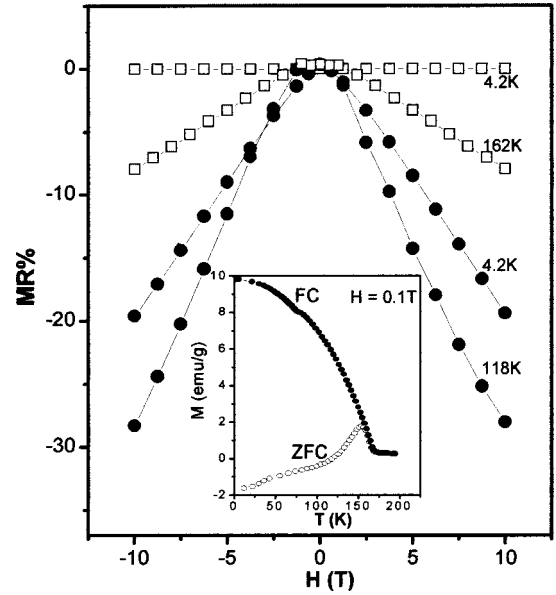

FIG. 3. Magnetoresistance as a function of field for SrRu$_{0.5}$Mn$_{0.5}$O$_3$ (solid symbols) along with the MR for the parent compound (open symbols). The inset shows the magnetization for SrRu$_{0.5}$Mn$_{0.5}$O$_3$ at $\mu_0 H = 0.1$ T under field-cooled (FC) and zero-field-cooled (ZFC) conditions.

low-spin Ru^{4+} ($S = 1$) and high-spin Mn^{4+} ($S = 3/2$), but is smaller than that for high-spin Ru^{5+} ($S = 3/2$) and high-spin Mn^{3+} ($S = 2$). This increased magnetic moment implies that a low-spin Ru(IV) and Mn(IV) should coexist with other high-spin valence states, namely, Mn(III):d^4 and Ru(V):d^3 states. Such a possibility could occur only if an oxidation-reduction reaction occurs between the Ru and Mn ions in order to maintain charge neutrality in the crystal lattice. We indeed observe such a signature for the existence of mixed valency in the XAS spectra, which will be discussed below.

C. Magnetotransport properties

Measurements of magnetotransport properties reveal that the parent compound SrRuO$_3$ shows a magnetoresistance (MR) ratio of the order of 10% near the $T_c \sim 160$ K at $\mu_0 H = 10$ T (Fig. 3), which agrees well with the reported value by Klein *et al.*[11] However, the MR ratio of SrRu$_{0.5}$Mn$_{0.5}$O$_3$ increases by 30% in the vicinity of the Curie temperature $T_c = 125$ K, which is 2 times higher than that of the parent compound (Fig. 3). This suggests that the enhancement in the MR ratio is due to the induced double-exchange (DE) interaction, which is more pronounced compared to the superexchange interaction. This is obvious since superexchange-mediated ferromagnetic compounds generally do not give rise to large MR ratios. The metallic nature of the ferromagnetic clusters persists up to 50 at. % of Mn in SrRuO$_3$ which could be due to the double-exchange ferromagnetic interaction since both Ru and Mn exist in the variable valence ionic state in SrRu$_{1-x}$Mn$_x$O$_3$. The double-exchange ferromagnetic interaction could be initiated between Mn^{3+}($t_{2g}^3 e_g^1$) and Mn^{4+}($t_{2g}^3 e_g^0$) or Ru^{5+}($t_{2g}^3 e_g^0$), which competes with the antiferromagnetic interaction be-

tween the two similar ions, resulting in the spin freezing behavior of the compound. This is evident from the difference in the zero-field-cooled (ZFC) and field-cooled (FC) magnetization curves below T_c as shown in the inset of Fig. 3, suggesting typical spin freezing behavior as observed in the double-exchange-mediated ferromagnetic compounds.[12,13] One of the reasons for the enhanced magnetoresistance is due to the presence of a large amount of weak-linked ferromagnetic and metallic clusters in the paramagnetic matrix, which are easily aligned by the magnetic field below the Curie temperature. In the presence of a magnetic field, the connectivity facilitates good current percolation between the clusters, opening up new conduction channels by the growing of ferromagnetic clusters and consequently a reduction in the resistivity. There is also prominent magnetoresistance of $SrRu_{0.5}Mn_{0.5}O_3$ at 4.2 K, and it is noted that the MR ratio varies linearly with the applied magnetic field (H). This indicates that the magnetotransport property at low temperature is an intrinsic phenomenon rather than extrinsic[14] and may originate from the spin freezing.

D. Mn $L_{2,3}$ XAS spectra

The determination of the valence states of the transition metals (TM's) using $L_{2,3}$ XAS spectra is well understood and has become a standard tool. Due to strong electronic correlations, the multiplet structure of the TM $L_{2,3}$ XAS spectrum can be well reproduced by an atomic multiplet or charge transfer multiplet calculation.[15] In Fig. 4 we present the Mn $L_{2,3}$ XAS spectra of the $SrRu_{1-x}Mn_xO_3$ system together with that of $LiMn_2O_4$ for comparison. The change in the spectral features with increasing Mn doping is similar to the changes observed for increasing Sr doping in $La_{1-x}Sr_xMnO_3$ series (see, for example, Abbate *et al.*[16]). The gradual shift to lower energy (Fig. 4) and the variation in the multiplet structure indicates a decrease in the Mn valence. The spectral feature of the tetravalent Mn compound $SrMnO_3$ is the same as observed by Abbate *et al.*,[16] but shows much better spectral resolution. The Mn L_3 edge shows many richer spectral features than the Mn L_2 edge. The dominant feature lies at 645 eV with a very narrow low-energy shoulder at 642.6 eV.

The Mn $L_{2,3}$ XAS spectrum of $SrRu_{0.5}Mn_{0.5}O_3$, which lies in the middle of the series, is almost identical to the spectrum of $LiMn_2O_4$, implying that the ground state of Mn corresponds to a mixed-valence state involving both the Mn(III)/Mn(IV) oxidation states. Park *et al.* have made such an inference recently for Co-doped $LaMn_{1-x}Co_xO_3$ compounds.[17] From $SrMnO_3$ to $SrRu_{0.5}Mn_{0.5}O_3$ the spectral weight transfers to lower energy, especially the features at 641.7 and 643 eV gain significant spectral weight. The shape of the spectra for the equiatomic Mn and Ru concentrations matches with that reported for $LaMnO_3$, where manganese predominantly exists in a Mn(III) oxidation state.[18]

E. Ru $L_{2,3}$ XAS spectra

Unlike the situation in $3d$ transition metals, the determination of the valence state of $4d$ transition metals is less
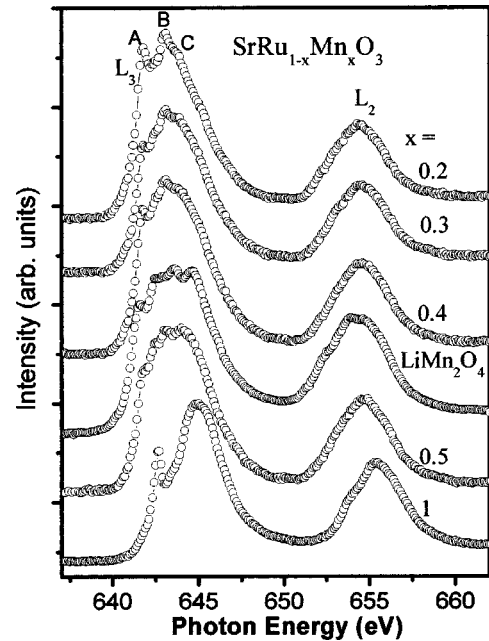

FIG. 4. Mn $L_{2,3}$ of Mn-doped $SrRu_{1-x}Mn_xO_3$, $0 \leqslant x \leqslant 0.5$. Peaks B and C corresponding to Mn(III) and Mn(IV) ions arise due to the transition from $2p$ core level to the final states $3d^4$ and $3d^3$, respectively. Note that the intensity of peak B decreases while peak C increases and 1:1 at $x=0.5$. This indicates that nearly equal concentrations of both the ions coexist in the ground state. The shape of the spectra and the chemical shift of the Mn $L_{2,3}$ XAS spectra of $SrRu_{0.5}Mn_{0.5}O_3$ are well matched to the reference compound $LiMn_2O_4$ where Mn exists both in Mn(III) and Mn(IV) oxidation states.

established.[19,20] In a recent work, although Ru in $RuSr_2GdCu_2O_8$ is proposed to be in a mixed-valence Ru (IV)/(V) state,[1] presence of such a charge distribution has not been verified. In order to understand the implications of the structural distortion and enhanced magnetic exchange in this solid solution, we attempt to probe the existence of a mixed valency in Ru and to correlate it with our results on the Mn valency. Before we discuss the detailed ground-state configuration of the Ru ions, we briefly compare the results of the parent $SrRuO_3$ (SR) and the equiatomic composition— namely, $SrRu_{0.5}Mn_{0.5}O_3$ (SRM50)—with a well-known tetravalent Ru compound RuO_2 and a pentavalent Ru compound $Sr_4Ru_2O_9$ (SR429) as shown in Fig. 5. To ease our comparison, we shift the L_2 spectra (open symbols) in each case, such that the high-energy feature (B) is aligned with the corresponding feature in the L_3 spectra (solid symbols). The L_2 spectra have also been multiplied by a factor of 2.15 in the case of both $4d^4$ systems. Peaks A and B are basically assigned to t_{2g}- and e_g-related states, respectively. The parent compound SR closely matches with tetravalent Ru(IV) oxide in RuO_2. This result is consistent with the result obtained from the effective magnetic moment calculation. The strong spin-orbit coupling constant λ for Ru^{4+} (800 cm^{-1}) and the electronic correlation effects inhibit the transition of the $2p \rightarrow t_{2g}$ related peak of $SrRuO_3$ at the L_2 edge.[21] SRM50 shows an increase in the spectral weight of the t_{2g}-related peak and a shift by 0.8 eV to higher energy, sug-
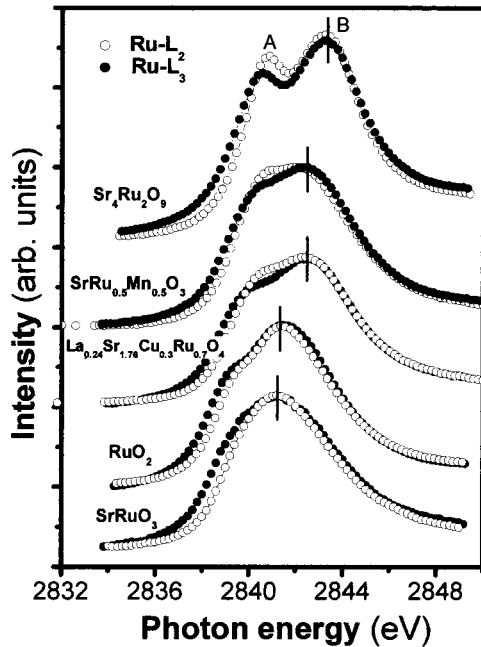
FIG. 5. Ru $L_{2,3}$ XAS spectra of $SrRu_{0.5}Mn_{0.5}O_3$ in comparison to the Ru (IV) and/or Ru (V) reference compound.

FIG. 6. Theoretical multiplet spectra at the L_3 (solid line) and L_2 (dashed line) edges for the (left panel) Ru $4d^4$ configuration and (right panel) for the Ru $4d^3$ configuration with reduced Slater integrals 40% and 15% of the atomic value, respectively. The values of the octahedral cubic crystal field 10 Dq used for both configurations are also given.

gesting a higher valency. However, these changes are only halfway with respect to the Ru(V) compound SR429. This implies that the valence of Ru in SRM50 could be in between the 4+ and 5+ states. The spectra of SRM50 indeed match well with $La_{0.24}Sr_{1.76}Cu_{0.3}Ru_{0.7}O_4$, with a Ru valency of 4.5. However, the metal-oxygen bond distance decreases upon Mn doping since the ionic radius of Mn(IV) (0.52 Å) is smaller than the ionic radius of Ru(IV) (0.63 Å) (Ref. 22) and hence the octahedral crystal field 10 Dq increases.

Previously, the differences of spectral features between Ru(IV) and Ru(V) have been intensively studied as a function of the Slater integrals. In order to exclude a possible influence of crystal field interactions upon Mn doping, we have simulated the $L_{2,3}$ XAS spectra for the $4d^4$ and $4d^3$ configurations as a function of 10 Dq using a crystal-field-multiplet calculation (CFMC).[23] We assumed the ground-state symmetry $3d^4$ ($t_{2g}^4 e_g^0$, with $^3T_{1g}$) with Slater integrals reduced to 40% at different octahedral crystal fields 10 Dq [Fig. 6(a)] and considering the ground-state symmetry $3d^3$ ($^4A_{2g}$) with reduced Slater integrals (15%) [Fig. 6(b)]. With a variation of the 10 Dq value from 1.8 to 2.8 eV for $4d^4$ and from 2.2 to 3.0 eV for $4d^3$ configurations, the basic spectral profiles do not change; e.g., the Ru L_3 (solid line) is more intense than Ru L_2 (dashed line) for $4d^4$ and becomes reversed for $4d^3$ and the energy shift is within 0.2 eV. Thus the observed spectral line shape as well as the chemical shift for SRM50 cannot be attributed to crystal field interactions, but to the Ru valence. Since the spectral line shape and the chemical shift are the same as the reference compound $La_{0.24}Sr_{1.76}Cu_{0.3}Ru_{0.7}O_4$, the effective average oxidation number of Ru observed is found to be 4.5.[24] Therefore we can conclude that in the SRM50 system, Ru exists as a redox pair involving Ru(IV) ($t_{2g}^4 e_g^0$, with $^3T_{1g}$ ground-state symmetry) and Ru(V) ($t_{2g}^3 e_g^0$, with $^4A_{2g}$ ground-state symme-
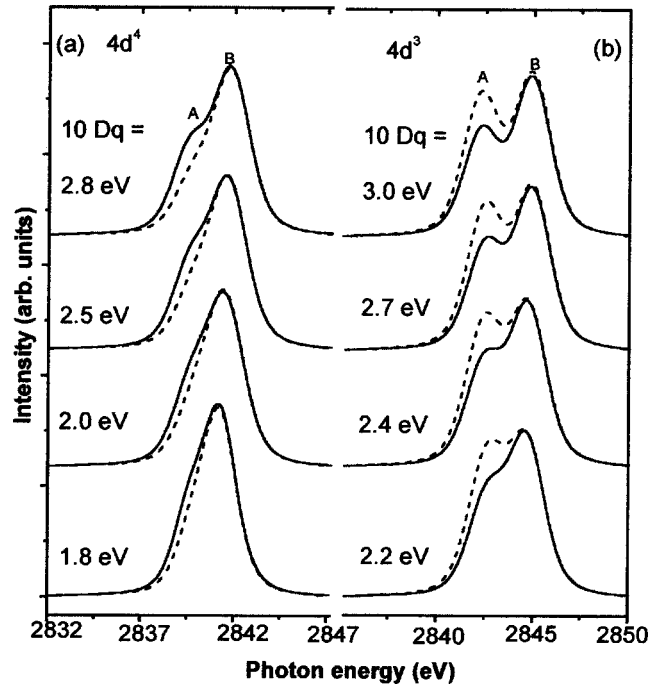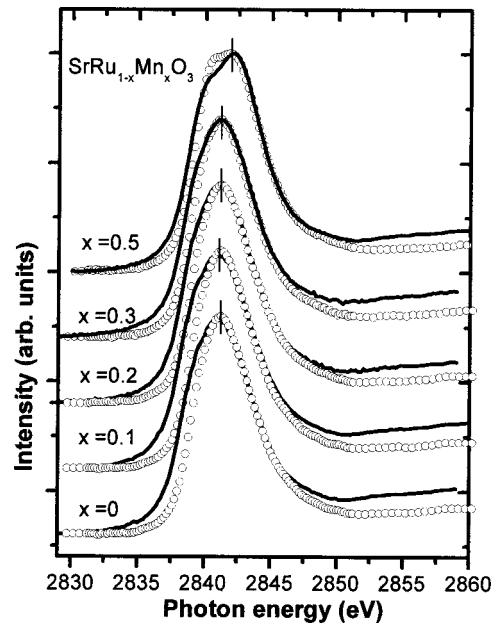

FIG. 7. Shows the Ru L_2 edge (open symbols) and Ru L_3 (solid line). The significant difference in the peak of A and the chemical shift for $SrRu_{0.5}Mn_{0.5}O_3$ at the L_2 and L_3 edges when compared to the parent compound $SrRuO_3$ indicates that a few percentage of Ru (IV) translates to Ru (V) on doping Mn ions.

try). Hence the mixed-valence Ru pair could be due to a possible redox reaction wherein Ru(IV) gets oxidized while Mn(IV) gets reduced such that a Mn(III)+Ru(V)↔Mn(IV) +Ru(IV) like charge redistribution occurs.

To verify the presence of the redox pair formation, we show in Fig. 7, the Ru $L_{2,3}$ XAS spectra of SrRu$_{1-x}$Mn$_x$O$_3$ series for various Mn doping levels, where one can see a significant change between $x=0.3$ and 0.5, while between $x=0$ and 0.3 the spectral change is marginal. This could be interpreted in comparison with our recent XAS results on Ru-substituted rare-earth perovskites,[7] where we observe that the Ru(V) state becomes predominant only with a higher proportion of Mn in the crystal lattice. It appears that this could be most likely due to the comparable reduction oxidation potential Ru(IV)/Ru(V) (1.07 eV) and Mn(III)/Mn(IV) (1.02 eV). To keep up with the charge neutrality, Mn(IV) gets reduced to an Mn(III) state as observed by the Mn $L_{2,3}$ edges, and Ru(IV) gets oxidized to the Ru(V) state. It is gratifying to note that during such a redox reaction, the depleting Mn(IV): $t_{2g}^3 e_g^0$ concentration, which is essential for DE mechanism, is ably compensated by the Ru(V): $t_{2g}^3 e_g^0$

ion. In such a charge distribution, the Mn(III) ion recognizes the Ru(V) ion as magnetically and chemically equivalent to the Mn(IV) ion.

IV. SUMMARY

In this study, we observe a unique magnetic pair making interaction between Mn and Ru ions in the Ru-O-Ru sublattice. The XAS spectra of Ru $L_{2,3}$ and Mn $L_{2,3}$ give supporting evidence for the structural and magnetic transitions observed in this solid solution. An unusual long-range ferromagnetic exchange mediated by a ionic pair involving Mn(III)+Ru(V)↔Mn(IV)+Ru(IV) shows that the Mn(III) ion recognizes Ru(V) as a magnetically and chemically equivalent Mn(IV) ion. This insight sets a reference for the role of Ru in manganites including the charge order manganites where Ru substitution displays novel properties.

*Author to whom correspondence should be addressed. FAX: 0512-59 7436. Electronic address: ssundar@iitk.ac.in

[1] Ken-ichi Kumagai, S. Takada, and Y. Furukawa, Phys. Rev. B **63**, 180509(R) (2001).

[2] M. Itoh, M. Shikano, and T. Shimura, Phys. Rev. B **51**, 16 432 (1995).

[3] Ranjan K. Sahu and S. Sundar Manoharan, Appl. Phys. Lett. **77**, 2382 (2000). See also S. Sundar Manoharan, R. K. Sahu, M. L. Rao, D. Elefant, and C. M. Schneider, Europhys. Lett. **59**, 451 (2002).

[4] P. V. Vanitha, A. Arulraj, A. R. Raju, and C. N. R. Rao, C. R. Acad. Sci. Paris 2 **11−13**, 595 (1999).

[5] A. Callagan, C. W. Moeller, and R. Ward, Inorg. Chem. **5**, 1572 (1966).

[6] A. Kanbayasi, J. Phys. Soc. Jpn. **41**, 1876 (1976).

[7] Ranjan K. Sahu, M. L. Rao, S. Sundar Manoharan, K. Dorr, and K.-H. Muller, Solid State Commun. **123**, 217 (2002).

[8] J. J. Randall and R. Ward, J. Am. Chem. Soc. **81**, 2629 (1959).

[9] P. A. Joy, S. K. Date, and P. S. Anil Kumar, Phys. Rev. B **56**, 2324 (1997).

[10] S. E. Livingstone, *The Chemistry of Ruthenium, Rhodium, Palladium, Osmium, Iridium and Platinum* (Pergamon, Oxford, 1973).

[11] L. Klein, J. S. Dodge, C. H. Ahn, T. H. Geballe, M. R. Beasley, and A. Kapitulnik, Phys. Rev. Lett. **77**, 2774 (1996); P. Kostic, N. C. Collins, Z. Schlesinger, J. W. Reiner, L. Klein, A. Kapitulnik, and T. H. Geballe, *ibid.* **81**, 2498 (1998).

[12] J. Blasco, J. Garcia, J. M. de Teresa, M. R. Ibarra, J. Perez, P. A. Algarabel, and C. Marquina, Phys. Rev. B **55**, 8905 (1997).

[13] J.-W. Cai, C. Wang, B.-G. Shen, J.-G. Zhao, and W.-S. Zhan, Appl. Phys. Lett. **71**, 1727 (1997).

[14] H. Y. Hwang, S.-W. Cheong, N. P. Ong, and B. Batlogg, Phys. Rev. Lett. **77**, 2041 (1996).

[15] Z. Hu, Chandan Mazumdar, G. Kandl, F. M. F. de Groot, S. A. Warda, and D. Reinen, Chem. Phys. Lett. **297**, 321 (1998).

[16] M. Abbate, F. M. F. de Groot, J. C. Fuggle, A. Fujimori, O. Strebel, F. Lopez, M. Domke, G. Kaindl, G. A. Sawatzky, M. Takano, Y. Takeda, E. Eisaki, and S. Uchida, Phys. Rev. B **46**, 4511 (1992).

[17] J.-H. Park, S.-W. Cheong, and C. T. Chen, Phys. Rev. B **55**, 11 072 (1997).

[18] F. M. F. de Groot, J. Fuggle, B. T. Thole, and G. A. Sawatzky, Phys. Rev. B **41**, 928 (1990).

[19] F. M. F. de Groot, Z. Hu, M. F. Lopez, G. Kaindl, F. Guillot, and M. Tronic, J. Chem. Phys. **101**, 6570 (1994).

[20] T. K. Sham, J. Am. Chem. Soc. **105**, 2269 (1983).

[21] Z. Hu, H. von Lips, M. S. Golden, J. Fink, G. Kaindl, F. M. F. de Groot, S. Ebbinghaus, and A. Reller, Phys. Rev. B **61**, 5262 (2000).

[22] R. D. Shannon and C. T. Prewitt, Acta Crystallogr., Sect. B: Struct. Crystallogr. Cryst. Chem. **25**, 925 (1969).

[23] F. M. F. de Froot, J. Fuggle, B. T. Thole, and G. A. Sawatzky, Phys. Rev. B **42**, 5459 (1990).

[24] S. Ebbinghaus, Z. Hu, and A. Reller, J. Solid State Chem. **156**, 194 (2001).